*Research Article*

# Assessment of Rotational Speed and Plunge Rate on Lap Shear Strength of FSSW Joints of AA7075/Mild Steel

**G. Ramya,**[1] **Subburam Pounrajan,**[2] **D. V. S. S. S. V. Prasad,**[3] **Sanjay Soni,**[4] **P. Ravichandran,**[5] **Koushik Kosanam,**[6] **Amara S. A. L. G. Gopala Gupta,**[7] **P. M. Dinesh,**[8] **Leevesh Kumar** ⓘ,[9] **and Bazani Shaik**[10]

[1]*Department of Mechanical Engineering, Rajalakshmi Engineering College, Chennai 602105, Tamil Nadu, India*
[2]*Department of Mechanical Engineering, Saveetha Engineering College, Chennai 602105, Tamil Nadu, India*
[3]*Department of Mechanical Engineering, Aditya College of Engineering, Surampalem 533437, Andhra Pradesh, India*
[4]*Department of Industrial and Production Engineering, Jabalpur Engineering College, Jabalpur 482011, Madhya Pradesh, India*
[5]*Department of Mechatronics Engineering, Kongu Engineering College, Erode 638060, Tamil Nadu, India*
[6]*Manufacturing Systems Engineering and Management, California State University, Northridge, CA 91325, USA*
[7]*Department of Computer Science and Engineering, Koneru Lakshmaiah Education Foundation, Vaddeswaram 522502, Andhra Pradesh, India*
[8]*Department of Electronics and Communication Engineering, Sona College of Technology, Salem 636005, Tamil Nadu, India*
[9]*Department of Construction Technology & Management, Ambo University, Ambo, Ethiopia*
[10]*Department of Mechanical Engineering, Ramachandra College of Engineering, West Godavari, Eluru 534007, Andhra Pradesh, India*

Correspondence should be addressed to Leevesh Kumar; leevesh.kumar@ambou.edu.et

Friction stir spot welding (FSSW) is an upgraded version of the friction stir welding process. This welding process can be used to replace permanent and temporary fastens such as bolts and nuts, screws, rivets, and welds. FSSW can be utilized to replace steel rivets in aircraft structure fabrication due to the elimination of time required to complete the joints and special tools. Moreover, the joining of dissimilar joints is very difficult due to the formation of different proportions of intermetallic compounds in the weld region. A lot of process parameters may influence the quality of the joints. This investigation analyzes the effect of speed of tool rotation and plunge rate of tensile shear fracture load of AA7075 mild steel dissimilar metal joints. From the observation, the joint fabricated with a speed of tool rotation of 1000 rpm and a plunge rate of 6 mm/min yielded a maximum shear fracture load of 9.86 kN. This weld strength enhancement may be linked to the formation of dynamic recrystallization and density distribution of strengthening precipitates.

## 1. Introduction

Dissimilar materials (such as aluminum and steel) fill the specific requirements in engineering applications, such as corrosion resistance and weight reduction. However, due to their manufacturing complexity, it is challenging to join them. These two alloys are difficult to be welded using fusion welding process [1]. The intermetallic compound is the major problem in the welding region. The intermetallic compound will reduce the joint strength due to its brittle nature. Solid-state technology is an ideal process to join such type of dissimilar materials. Friction stir welding (FSW) is one of the processes to join similar and dissimilar materials [2]. FSW eliminates all the fusion welding problems. Rivets, bolts and nuts, and screws were used as mechanical elements to join dissimilar materials. Due to the large tool requirement, the riveting process consumes more time than other joining processes [3]. The friction stir spot welding (FSSW)

is an alternate method to replace permanent joints such as rivets. Chowdhury et al. [4] spot welded AZ31B and AA5754 with 2 mm thickness using the FSSW technique. A left hand threaded pin of 5 mm diameter was used in this research work. FSSW was developed by Chun et al. [5] using a tool constructed of tool steel and consisting of a shank, shoulder, and pin to join aluminum and the AZ31 alloy. The shoulder diameter and pin diameter were 13.5 mm and 9.5 mm, respectively. The thickness of the intermetallic layer rose as the speed of tool rotation and time duration increased, and this had a substantial impact on the joint strengths. The Al and Mg alloy joint's maximum tensile shear fracture load (TSFL) was at 1.5 kN. However, as the speed of rotation and the holding time were increased beyond the maximum value, the TSFL fell. Using a tapered pin tool, Freeney et al. [6] investigated the effects of plunge depth, plunge rate, and speed of tool rotation on the TSFL of AA5052 and discovered that a low rotational speed created a bigger weld interface, resulting in increased weld strength. With 1 mm thick sheets, the TSFL was found to be 4.2 kN, and with 1.6 mm sheets, it was around 5 kN. Shen et al. [7] designed a steel tool with a 12 mm shoulder diameter and a concave profile to connect AA6061 alloy sheets of 2 mm thickness, and joints were produced at a greater tool speed and lesser dwell periods. Tozaki et al. [8] utilized a shoulder diameter of 8 mm to join 1.5 mm thick sheets using a different pin. Moreover, the formation of microstructure in the FSSW joints purely depends on the pin geometry and process parameters. From the experimental results, the TSFL value increases with increasing the pin length.

Welds on 1 mm thick AA6111 and steel sheets were reported by Chen and Yazdanian [9], who used a steel tool with a shoulder diameter of 10 mm, a probe of 3 mm diameter, and a 1.5 mm length probe with a scroll profile to optimize material flow. Sun et al. [10] reported the FSSW of AA6061 and steel. The pin length has minimal influence on the weld characteristics, with a maximum TSFL of 3607 N. Boz and Kurt [11] used a tungsten rhenium alloy tool to attach 1.0 mm thick AA6016 to a 2.0 mm thick galvanized sheet and found that the IMC layer thicknesses increase with changing the speed of tool and penetration. FSSW of steel sheets of 1 mm thickness with AA5754 sheets of 2 mm thickness was reported by Finger et al. [12]. They discovered that, by joining the right spindle speed and dwell duration, FSSW strength may be greatly increased. By raising the dwell duration to an optimum level, a TSFL of 8.4 kN per spot was reached in the shear tension test. FSSW of advanced steel with AA6061 was carried out by Chen et al. [13]. The wider metallurgical bonding at the nugget zone and optimum formation of the hook on both sides were the reasons for the superior strength. Furthermore, a keyhole refill of FSSW on AA6061 with TRIP steel was carried out. Three distinct grain structures were observed in the hook region [14]. Kumamoto et al. [15] analyzed the fatigue and microstructural behavior of FSSW aluminum and steel dissimilar materials. The test result showed that the joint had an optimum hook at the interface between the steel and aluminum alloy due to high flow of aluminum alloy.

From the literature survey, it is understood that a lot of work has been carried out in dissimilar materials. The FSSW of dissimilar materials (AA7075 with mild steel) is very scanty. Hence, this investigation focuses on the influence of tool rotation speed and plunge rate on the TSFL of AA7075 with mild steel.

## 2. Experimental Work

AA7075 aluminum alloy and mild steel were selected as the base material in this work. The BM's chemical composition and mechanical properties are presented in Tables 1 and 2. Both AA7075 and mild steel are mainly used in heavy structural fabrication industries in different configurations due to their high strength and weight reduction. The specimens were cut from a 300 mm × 300 mm × 2 m sheet. A DoALL machine was used to cut the required size for FSSW, and the joint configuration is as shown in Figure 1(a). A CNC-FSW machine was used for welding the dissimilar materials (Figure 1(b)). The fabricated joints are shown in Figure 1(c). The microstructure of both BM is presented in Figures 1(d) and 1(e). Table 3 shows the design of the experiments by considering the selected process parameters. The orientation of grains in both materials was coarse and elongated. Tensile shear fracture load (TSFL) of AA7075/MS was performed in the universal tensile machine (UTM). A light optical microscope was used to distinguish the formation of grains in various weld regions. Moreover, the specimen was sliced across the transverse cross section of the nugget to measure the hardness. A scanning electron microscope was used to identify the type of fracture mode. A Vickers microhardness tester with a load of 0.50 N and a dwell time of 15 sec was used.

## 3. Results and Discussion

*3.1. Influence of Rotational Speed of Tool on TSFL.* The tensile tests show that tool rotation speed has a noteworthy influence on the TSFL of the joints as presented in Table 4. The TSFL of the joints rises and then falls when the speed of tool rotation is raised from 800 to 900 rpm. The joint with the highest TSFL of 9.46 kN was made at a rotating tool speed of 900 rpm. At an 800-rpm tool rotation speed, the joint had the lowest TSFL of 6.12 kN. Table 4 shows the effect of the speed of tool rotation on the geometrical features of equally sectioned FSSW joints. The macrographs were used to compute the hook height (HH), hook width (HW), and hook initiation distance (HID) from the tool interface. Regardless of the process condition, an increase in HW increases the TSFL, although an increase in HH reduces the TSFL. The HID from the joint contact increases as the TSFL increases, with a few exceptions. Hardness profiles and microhardness values for various tool revolving speeds are shown in Figure 2. From the hardness profiles, the following inferences may be drawn: the rotation tool speed impacts the toughness of the welds. The highest hardness is recorded around the keyhole, regardless of tool rotation rates. The lowest hardness of the joint is measured at the interface of the TMAZ and HAZ areas, regardless of tool rotation speeds. When the rotating tool speed is increased from 800 to 900 rpm, the microhardness of the NZ increases and then decreases as the

TABLE 1: Chemical composition of AA7075/MS.

| Elements | C | Si | Al | Cr | Cu | Mn | Ni | P | Mg | Fe |
|---|---|---|---|---|---|---|---|---|---|---|
| AA7075 | — | 0.5 | 95.8 | 0.04 | 0.35 | 0.15 | — | — | 0.8 | 0.7 |
| MS | 0.09 | — | — | — | — | 0.22 | — | 0.009 | — | Bal. |

TABLE 2: Mechanical properties of AA7075/MS.

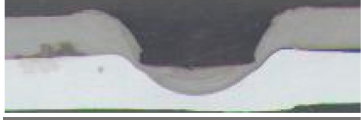| Materials | 0.2% Y.S (MPa) | UTS (MPa) | Elongation (%) | Microhardness (HV) |
|---|---|---|---|---|
| AA7075 | 281 | 308 | 16 | 107 |
| MS | 270 | 350 | 18 | 346 |
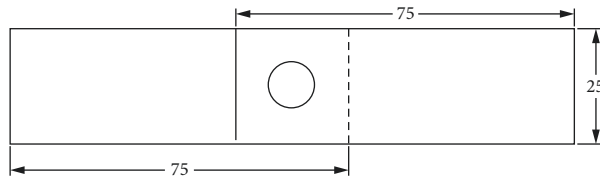


(a)



(b)
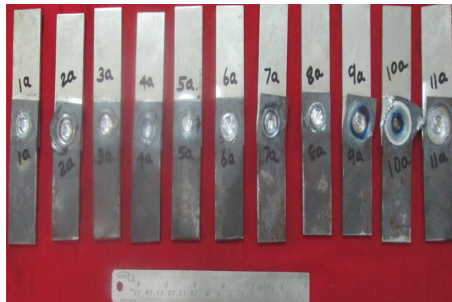


(c)
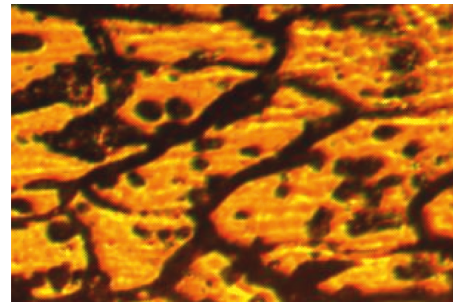


(d)
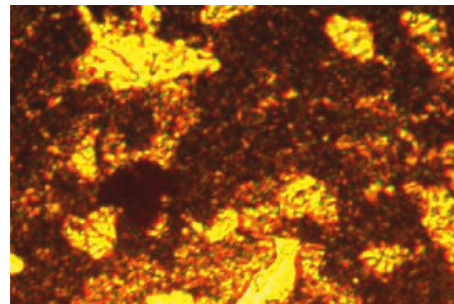


(e)

FIGURE 1: (a) FSSW joint configuration and photographs of the (b) FSW machine and (c) fabricated joints. Optical micrograph of (d) AA7075 and (e) mild steel.

TABLE 3: Design matrix and its response.

| | $N$ (rpm) | $R$ (mm/min) | $T$ (sec) | $D$ | |
|---|---|---|---|---|---|
| | 800 | 4 | 5 | 3 | 6.12 |
| | 850 | 4 | 5 | 3 | 7.45 |
| Speed of tool rotation ($N$) | 900 | 4 | 5 | 3 | 9.46 |
| | 950 | 4 | 5 | 3 | 8.56 |
| | 1000 | 4 | 5 | 3 | 7.21 |
| | 900 | 2 | 5 | 3 | 8.31 |
| | 900 | 3 | 5 | 3 | 8.42 |
| Rate of plunge ($R$) | 900 | 4 | 5 | 3 | 8.89 |
| | 900 | 5 | 5 | 3 | 7.28 |
| | 900 | 6 | 5 | 3 | 6.81 |

TABLE 4: Influence of speed of tool rotation on the macrograph.

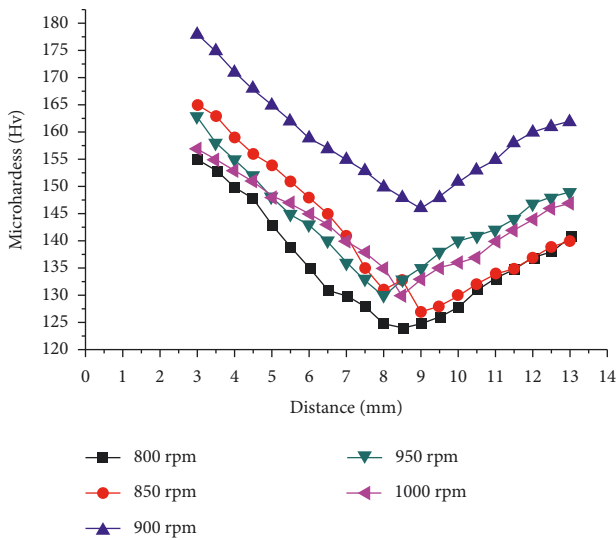| Speed of tool rotation | Macrostructure | Observation |
| --- | --- | --- |
| 800 |  | TSFL = 6.12 kN; HH = 1.52 mm; HW = 1.25 mm; HID = 2.14 mm; ABVHTP = 156.23 mm$^3$ |
| 850 |  | TSFL = 7.18 kN; HH = 1.48 mm; HW = 1.28 mm; HID = 2.45 mm; ABVHTP = 161.21 mm$^3$ |
| 900 |  | TSFL = 9.46 kN; HH = 1.44 mm; HW = 1.35 mm; HID = 2.95 mm; ABVHTP = 165.02 mm$^3$ |
| 950 |  | TSFL = 8.12 kN; HH = 1.51 mm; HW = 1.30 mm; HID = 2.88 mm; ABVHTP = 158.52 mm$^3$ |
| 1000 |  | TSFL = 7.21 kN; HH = 1.63 mm; HW = 1.25 mm; HID = 2.65 mm; ABVHTP = 155.23 mm$^3$ |


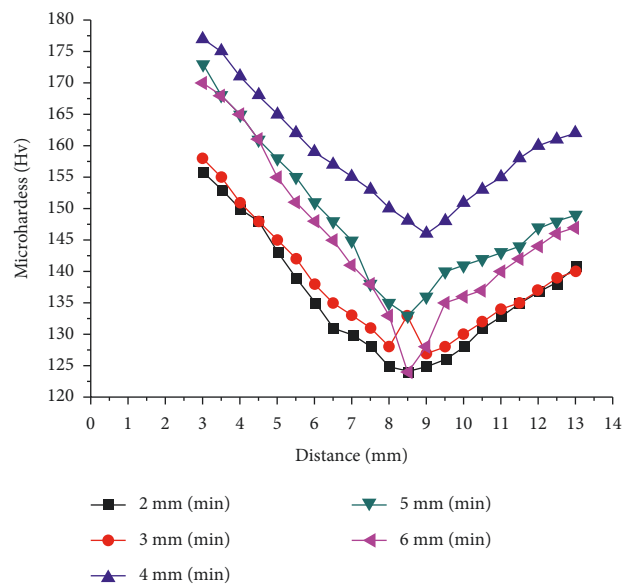
FIGURE 2: Effect of tool rotational speed on the hardness profile.



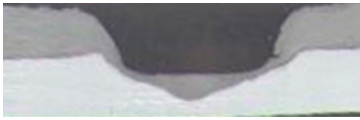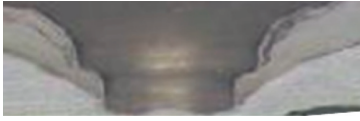FIGURE 3: Effect of plunge rate on the hardness profile.

speed of tool rotation is increased further. The NZ microhardness of the joint fabricated at a speed of tool rotation of 900 rpm is 178 HV. The NZ hardness of the joint fabricated at an 800-rpm tool rotational speed was 155 HV. Figure 3 shows optical micrographs of symmetrically sectioned joints produced at various tool rotation speeds. As seen in the micrographs, the tool rotation speed significantly influences the final grain size at the SZ, TMAZ, and HAZ. All joint stir zones completely change coarse and elongated base-metal grains into refined equiaxed grains. The grains in the TMAZ area are long, have an inclined orientation, and are coarser in size than those in the stir zone at all joints. The grains in HAZ are equiaxed, similar to those in the stir zone, but they are more significant. Regardless of SZ, TMAZ, or HAZ, grain

size reduces when the rotation of tool speed improves to a certain extent. Excellent and recrystallized grains can be seen in the NZ of the joint formed at 900 rpm.

The fracture surface analysis can lead to the following conclusions: the rate at which a tool spins has a significant influence on the failure mechanism of FSSW joints. A "partially curved" failure mechanism may be seen on the shattered surface of a joint created at tool rotation rates of 800, 850, and 950 rpm. On the fractured surface of a joint created at 1000 rpm tool rotation speed, the "eyelet" failure mechanism is discernible. On the broken surface of a joint made with a speed of tool rotation of 900 rpm, the "nugget

TABLE 5: Influence of the rate of plunge on TSFL of dissimilar FSSW joints.

| Rate of plunge (mm/min) | Macrograph | Observation |
| --- | --- | --- |
| 2 |  | TSFL = 7.06 kN; HH = 1.52 mm; HW = 1.82 mm; HID = 2.13 mm; ABVHTP = 128.74 mm$^3$ |
| 3 |  | TSFL = 7.23 kN; HH = 1.44 mm; HW = 2.01 mm; HID = 2.41 mm; ABVHTP = 142.21 mm$^3$ |
| 4 |  | TSFL = 9.46 kN; HH = 1.40 mm; HW = 2.24 mm; HID = 3.209 mm; ABVHTP = 148.45 mm$^3$ |
| 5 |  | TSFL = 8.89 kN; HH = 1.31 mm; HW = 2.10 mm; HID = 2.74 mm; ABVHTP = 142.21 mm$^3$ |
| 6 |  | TSFL = 8.44 kN; HH = 1.52 mm; HW = 1.82 mm; HID = 2.21 mm; ABVHTP = 135.01 mm$^3$ |

pull-out" kind of failure may be noticed. The increased tool rotational speed boosts the peak temperature, which raises the NZ volume, but successive increases in the tool rotational speed have little influence on the NZ volume. Gerlich et al. [16] found that an increase in the speed of tool rotation had no influence on the quantity of heat produced since the torque is reduced and the NZ breadth and volume did not change much. Despite the lower peak temperature accompanied by a faster cooling rate, poor heat input and insufficient stirring action (inadequate plasticization) result in a coarser grain structure in the stir zone at lower tool rotation speeds. Increased rotational speeds result in higher heat input and the generation of coarse grains in the NZ due to a higher peak temperature coupled with a slower cooling rate. At a speed of tool rotation of 900 rpm, the low peak temperature produced finer granules in the NZ. The equiaxed grains in the NZ were most likely formed by agitating and recrystallizing plasticized materials. In the NZ of FSW, Liu et al. [17] discovered the production of equiaxed grains. It is also important to note that the high heat input is only used to expand the HAZ's width, not the NZ volume. Even though the cycle time is the same everywhere, differences in rotational speed cause material swirling and mixing around the spinning pin, as well as fluctuations in peak temperature output [18]. This affects the amount of heat given to the welded sheets as well as the forging force. The axial force is reduced by increasing the tool rotating speed, resulting in mere consolidation of the plasticized material between the bottom and top sheets, and a smaller region of complete bond in the NZ [19]. Despite the fact that the forging force is greater at lower tool rotation speeds, inadequate heat generation leads to the limited hardness at the stir zone. The size of the true nugget grows as the tool rotation speed increases for a certain probe length [20]. The tensile shear strength

increases under tensile shear stress as the nugget diameter increases, thereby enhancing the area.

### 3.2. Influence of Plunge Rate on TSFL.

The TSFL of FSSW AA7075 with carbon steel alloy joints generated at various plunging rates is presented in Table 5. The tensile test findings can be used to infer the following conclusions: the plunge rate impacts the FSSW joint's tensile strength. The joint's tensile strength improves when the plunge rate is increased from 2 to 4 mm/min and then declines. The joint with the highest TSFL of 9.46 kN was made at a 4 mm/min plunge rate. The joint with the lowest TSFL of 7.06 kN was made at a plunge rate of 2 mm/min. Macrographs are used to determine HH, HW, and HID distances from the tool interface. It is also worth noting that, by increasing HW, TSFL increases independent of process condition, but by increasing HH, TSFL decreases. The HID from the tool influence region of the joints rises as the TSFL increases, with a few exceptions. With values of HH and HW of 1.40 mm and 2.24 mm, respectively, the joint manufactured at a plunge rate of 4 mm/min had the greatest TSFL, whereas the plunge rate of 2 mm/min had the lowest TSFL, with values of HW and HH of 1.52 mm and 1.82 mm, respectively. Microhardness values at various plunging rates are shown in Figure 4. The plunge rate significantly influences the weld hardness, as can be observed from the hardness profile. The most excellent hardness is determined around the keyhole, regardless of the plunge rates used (inside the stir zone). The minimum hardness of the joint is assessed at the interface of the HAZ and TMAZ regions, regardless of the plunge rates used. When the dive rate is increased from 2 mm/min to 4 mm/min, the microhardness of the NZ increases; then, it decreases as the plunge rate is increased further. The joint

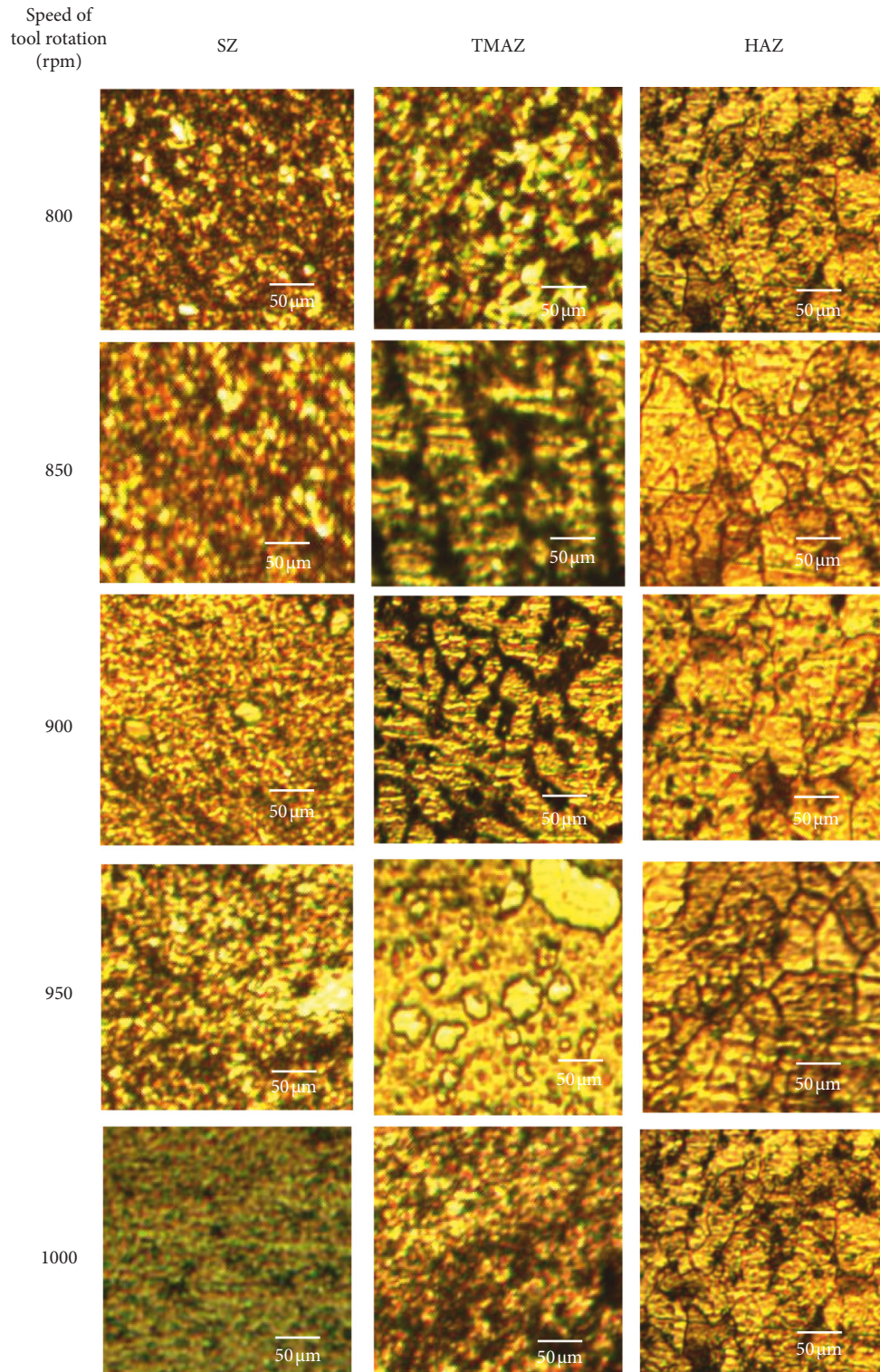| Speed of tool rotation (rpm) | SZ | TMAZ | HAZ |
|---|---|---|---|
| 800 | | | |
| 850 | | | |
| 900 | | | |
| 950 | | | |
| 1000 | | | |



FIGURE 4: Influence of tool rotational speed on the microstructure.

with the highest NZ microhardness of 177 HV was made at a 4 mm/min plunge rate. NZ microhardness of the mutual welding zone generated at a plunge rate of 2 mm/min was the lowest, i.e., 156 HV.

Figure 5 shows optical micrographs of FSSW joints produced at various plunging rates. The plunge rate has a considerable influence on the final grain size at SZ, TMAZ, and HAZ, as seen in the micrographs. All joints' NZ completely changed the coarse and elongated base metal grains into refined equiaxed grains. The grains in the TMAZ area are elongated, have an inclined orientation, and are coarser in size than those in the NZ at all joints. The grains in
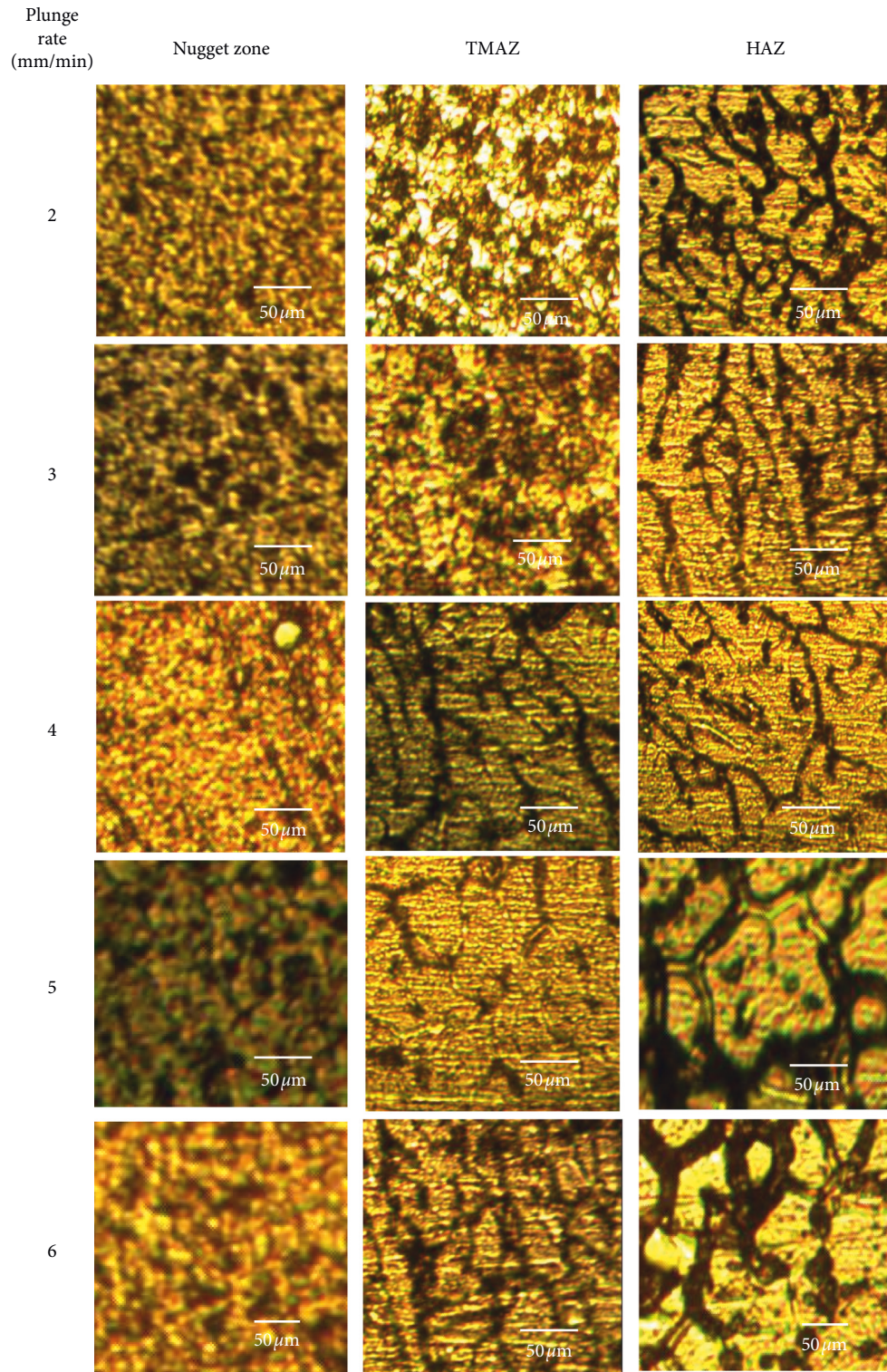
FIGURE 5: Influence of plunge rate on the microstructure.

HAZ are equiaxed, similar to those in the NZ, but are more extensive. The size of grains in the NZ of the joint formed at 4 mm/min is excellent. Grain size is more extensive in the NZ of joints produced at varying plunging rates [21]. The shattered surfaces of lap shear tested samples were scanned with a digital scanner and analyzed using an SEM to better understand the failure pattern. The fractured areas of the joints formed at 2 mm/min, 5 mm/min, and 6 mm/min suggest a "partially curved" mode of failure, as per the fractograph. On the shattered area of a joint produced at a plunging rate of 4 mm/min, the "nugget pull-out" kind of failure occurred. The fracture surface of a joint made at a

3 mm/min plunging rate demonstrates the "nugget debonding" kind of failure [22]. In contrast to the other parameters, increasing the plunge rate reduces the heat input. The cycle time is shorter when the plunge rate is more remarkable, while the cycle duration is longer whenever the plunge rate is lower. High maximum temperatures are observed at lower plunge rates, resulting in more heat input. The enhanced stirring force generated by the longer cycle length resulted in a coarser grain structure in the NZ. The low peak temperature combined with the intense heat input results in an inadequate stirring activity at higher plunge rates, resulting in a coarse grain structure in the NZ. A combination of high temperature at low plunge rates and a longer axial force duration produced more refined grains in the NZ. A decrease in the dislocation density and precipitate dispersion can explain the difference in material softening between the SZ and the BM [23]. In addition, the plunge rate affects the hardness of the weldment as well as the joint's performance. The duration of the forging force is shortened with a faster plunging rate, resulting in inadequate material consolidation between the top and bottom sheets and a weld nugget with a lessened complete metallurgical bond. The hardness of the NZ is determined by the peak temperature, torque, and magnitude retention, which varies with plunge rates. The strength of the joints varied depending on the cycle time, heat input, and axial force across the site. Lower plunge rates resulted in a bigger TSFL in certain studies, such as the study conducted by Fereiduni et al. [24]; however, this varied depending on the rotational speeds used.

## 4. Conclusions

The FSSW technique is used for joining dissimilar materials successfully. The essential points are derived from the experimental work as follows:

(1) The FSSW is carried out using predominant process parameters such as the rotational speed and rate of the plunge to predict the tensile shear fracture load of dissimilar materials (AA7075/MS).

(2) The joint welded with the rotational speed of 1200 rpm, plunge rate of 5 mm/min, dwell time of 5 sec, and diameter ratio of 3 was found to have higher TSFL.

(3) An optimum process parameter could achieve the maximum TSFL of 9.43. This could be achieved with the correct material flow by the optimum heat input during the FSSW process.

(4) The eyelet fracture mode is obtained by recrystallized grains in the nugget zone. This suggests that the fracture type is ductile.

(5) The hook initiation distance from the tool influence region of the joints increases as the TSFL increases, with a few exceptions. With values of HH and HW of 1.40 mm and 2.24 mm, respectively, the joint manufactured at a plunge rate of 4 mm/min had the greatest TSFL.

(6) However, the plunge rate of 2 mm/min had the lowest TSFL, with values of HW and HH of 1.52 mm and 1.82 mm, respectively.

## Data Availability

The data used to support the findings of this study are included within the article.

## Disclosure

The publication of this research work is only for academic purposes.

## Conflicts of Interest

The authors declare that they have no conflicts of interest regarding the publication of this paper.

## References

[1] Y. Nakashima, H. Hiramatsu, K. Michiba, and M. Fujimoto, "Prediction of joint performance of friction spot joining by finite element analysis (report 1) - experimental study for modeling of friction spot joining," in *Proceedings of the Preprints of the National Meeting of Japan Welding Society*, Tokyo, Tokyo, Japan, September 2004.

[2] A. Gerlich, P. Su, and T. H. North, "Peak temperatures and microstructures in aluminium and magnesium alloy friction stir spot welds," *Science and Technology of Welding & Joining*, vol. 10, no. 6, pp. 647–652, 2005.

[3] M. Merzoug, M. Mazari, L. Berrahal, and A. Imad, "Parametric studies of the process of friction spot stir welding of aluminium 6060-T5 alloys," *Materials & Design*, vol. 31, no. 6, pp. 3023–3028, 2010.

[4] S. Chowdhury, D. L. Chen, S. D. Bhole, X. Cao, and P. Wanjara, "Lap shear strength and fatigue behavior of friction stir spot welded dissimilar magnesium-to-aluminum joints with adhesive," *Materials Science and Engineering A*, vol. 562, pp. 53–60, 2013.

[5] C. Chun, W. Chang, and H. Cho, "Study on friction spot joining of light metal for automotive," *Preprints of the National Meeting of Japan Welding Society*, pp. 72–76, 2006.

[6] T. A. Freeney, S. R. Sharma, and R. S. Mishra, "Effect of welding parameters on properties of 5052 Al friction stir spot welds," *SAE Technical Paper Series*, in *Proceedings of the SAE 2006 World Congress & Exhibition*, Detroit, Michigan, September 2006.

[7] Z. Shen, X. Yang, Z. Zhang, L. Cui, and Y. Yin, "Mechanical properties and failure mechanisms of friction stir spot welds of AA 6061-T4 sheets," *Materials & Design*, vol. 49, pp. 181–191, 2013.

[8] Y. Tozaki, Y. Uematsu, and K. Tokaji, "Effect of tool geometry on microstructure and static strength in friction stir spot welded aluminium alloys," *International Journal of Machine Tools and Manufacture*, vol. 47, no. 15, pp. 2230–2236, 2007.

[9] Z. W. Chen and S. Yazdanian, "Friction Stir Lap Welding: material flow, joint structure and strength," *Journal of Achievements in Materials and Manufacturing Engineering*, vol. 55/2, pp. 629–637, 2012.

[10] Y. F. Sun, H. Fujii, N. Takaki, and Y. Okitsu, "Microstructure and mechanical properties of dissimilar Al alloy/steel joints

prepared by a flat spot friction stir welding technique," *Materials & Design*, vol. 47, pp. 350–357, 2013.

[11] M. Boz and A. Kurt, "The influence of stirrer geometry on bonding and mechanical properties in friction stir welding process," *Materials & Design*, vol. 25, no. 4, pp. 343–347, 2004.

[12] G. Figner, R. Vallant, T. Weinberger, N. Enzinger, H. Schröttner, and H. Paśič, "Friction stir spot welds between aluminium and steel automotive sheets: influence of welding parameters on mechanical properties and microstructure," *Welding in the World*, vol. 53, no. 1-2, pp. R13–R23, 2009.

[13] K. Chen, X. Liu, and J. Ni, "Friction stir resistance spot welding of aluminum alloy to advanced high strength steel," *Journal of Manufacturing Science and Engineering*, vol. 140, no. 11, Article ID 111007, 2018.

[14] K. Chen, X. Liu, and J. Ni, "Keyhole refilled friction stir spot welding of aluminum alloy to advanced high strength steel," *Journal of Materials Processing Technology*, vol. 249, pp. 452–462, 2017.

[15] K. Kumamoto, T. Kosaka, T. Kobayashi, I. Shohji, and Y. Kamakoshi, "Microstructure and fatigue behaviors of dissimilar a6061/galvannealed steel joints fabricated by friction stir spot welding," *Materials*, vol. 14, no. 14, p. 3877, 2021.

[16] P. Gerlich, A. Su, T. H. North, and G. J. Bendzsak, "Energy utilization and generation during friction stir spot welding," *Science and Technology of Welding & Joining*, vol. 11, no. 2, pp. 163–169, 2006.

[17] H. J. Liu, H. Fujii, M. Maeda, and K. Nogi, "Mechanical properties of friction stir welded joints of 1050 - H24 aluminium alloy," *Science and Technology of Welding & Joining*, vol. 8, no. 6, pp. 450–454, 2003.

[18] C. Genevois, A. Deschamps, A. Denquin, and B. Doisneaucottignies, "Quantitative investigation of precipitation and mechanical behaviour for AA2024 friction stir welds," *Acta Materialia*, vol. 53, no. 8, pp. 2447–2458, 2005.

[19] J. F. Henrichs, C. B. Smith, B. F. Orsini, R. J. DeGeorge, B. J. Smale, and P. C. Ruehl, "Friction stir welding for the 21st century automotive industry," in *Proceedings of the 5th International Symposium of Friction Stir Welding*, Metz, France, September 2004.

[20] Y. Tozaki, Y. Uematsu, and K. Tokaji, "A newly developed tool without probe for friction stir spot welding and its performance," *Journal of Materials Processing Technology*, vol. 210, no. 6-7, pp. 844–851, 2010.

[21] M. K. Belichi, A. Irfan Yukler, and M. Kurtulmulus, "Optimizing welding parameters friction stir spot weld of high density poly ethylene sheet," *Materials and Design*, vol. 32, pp. 4074–4079, 2011.

[22] X. Song, L. Ke, L. Xing, F. Liu, C. Huang, and C. Huang, "Effect of plunge speeds on hook geometries and mechanical properties in friction stir spot welding of A6061-T6 sheets," *International Journal of Advanced Manufacturing Technology*, vol. 71, no. 9-12, pp. 2003–2010, 2014.

[23] N. T. Nguyen, D.-Y. Kim, and H. Y. Kim, "Assessment of the failure load for an AA6061-T6 friction stir spot welding joint," *Proceedings of the Institution of Mechanical Engineers - Part B: Journal of Engineering Manufacture*, vol. 225, no. 10, pp. 1746–1756, 2011.

[24] E. Fereiduni, M. Movahedi, and A. H. Kokabi, "Aluminum/steel joints made by an alternative friction stir spot welding process," *Journal of Materials Processing Technology*, vol. 224, pp. 1–10, 2015.